

Crystal-field excitations and spin-phonon interactions in DyNi₂B₂C: Raman scattering study

Heesuk Rho*

*Department of Physics, Research Institute of Physics and Chemistry, Chonbuk National University, Jeonju 561-756, Korea and
Department of Physics and Frederick Seitz Materials Research Laboratory, University of Illinois at Urbana-Champaign,
Urbana, Illinois 61801, USA*

Miles V. Klein

*Department of Physics and Frederick Seitz Materials Research Laboratory, University of Illinois at Urbana-Champaign,
Urbana, Illinois 61801, USA*

Paul C. Canfield

Ames Laboratory, Department of Physics and Astronomy, Iowa State University, Ames, Iowa 50011, USA

(Received 24 June 2010; published 27 August 2010)

We report polarized Raman results of magnetic superconductor DyNi₂B₂C ($T_c=6.2$ K, $T_N=10.3$ K) to explore crystal-field (CF) excitations and spin-phonon interactions. In addition to the Ni- B_{1g} phonon mode at 199 cm⁻¹, we observed additional Raman modes at 124, 151, and 221 cm⁻¹. By careful analysis of the temperature evolution of these modes, we attribute the 124 cm⁻¹ excitation to a CF transition. The 151 and 221 cm⁻¹ modes correspond to zone-folded phonons because they are completely quenched for $T > T_N$. With increasing temperature across T_N , the 124 cm⁻¹ excitation diminishes rapidly in intensity and, interestingly, an additional mode appears at 119 cm⁻¹. This excitation grows in intensity with increasing temperature toward 50 K and gradually decreases with increasing temperature further. We attribute the 119 cm⁻¹ excitation to an excited CF transition from a low-lying CF level at 5 cm⁻¹ to the higher CF level at 124 cm⁻¹. Anomalous temperature-dependent behavior of the Ni- B_{1g} phonon mode was observed in peak energy and in spectral width, i.e., both the phonon energy and the linewidth are enhanced in the vicinity of T_N , suggesting the presence of strong spin-phonon interactions near the antiferromagnetic ordering temperature in DyNi₂B₂C.

DOI: [10.1103/PhysRevB.82.064423](https://doi.org/10.1103/PhysRevB.82.064423)

PACS number(s): 75.30.-m, 78.30.-j, 74.70.Dd, 71.70.Ch

I. INTRODUCTION

The local order of magnetic moments strongly correlates with superconductivity in rare-earth-bearing compounds, such as $RMo_5(S,Se)_8$, RRh_4B_4 , and RNi_2B_2C (R = rare-earth ion).¹ Rare-earth nickel borocarbide compounds RNi_2B_2C provide a useful means of understanding the interplay between superconductivity and magnetism. For $R=Dy, Ho, Er,$ and Tm , superconductivity can coexist with antiferromagnetic (AF) order.¹⁻⁵ Among these compounds, DyNi₂B₂C exhibits some unique properties in its magnetic structures. For instance, DyNi₂B₂C becomes a superconductor ($T_c=6.2$ K) below the AF ordering temperature ($T_N=10.3$ K).² For RNi_2B_2C ($R=Ho, Er, Tm$), AF order appears below T_c .³⁻⁵ The crossover between the $T_c > T_N$ regime and the $T_N > T_c$ regime occurs between HoNi₂B₂C and DyNi₂B₂C. For rare-earth nickel borocarbide compounds, both T_N and T_c are scaled by the de Gennes factor, i.e., T_N and the suppression of T_c exhibit linear dependence on the de Gennes factor.¹ Interestingly, detailed study of Ho_{1-x}Dy_xNi₂B₂C has revealed that dependence of T_c on the de Gennes factor disappears for $T_c < T_N$.⁶ Unlike RNi_2B_2C ($R=Ho, Er, Tm$) which exhibit local extrema in the temperature-dependent upper critical field $H_{c2}(T)$, DyNi₂B₂C exhibits a linear monotonic decrease in $H_{c2}(T)$ with increasing temperature.^{2,4,5,7,8} Magnetic correlations in RNi_2B_2C manifest themselves as large anisotropic magnetic susceptibilities at low temperature and as Schottky anomalies in specific-heat measurements.^{2-5,9} Therefore, rare-earth elements in RNi_2B_2C play a crucial role in the interplay be-

tween magnetism and superconductivity. The magnetic properties of these compounds are strongly influenced by the rare-earth sublattice and are closely related to the crystal-field (CF) interactions.^{10,11} CF energy levels can be used to calculate CF parameters and, as a result, provide useful information on the magnetic properties such as magnetic susceptibility¹² and the Schottky specific heat.¹³

CF excitations can be directly probed using experimental methods such as Raman scattering,¹⁴ inelastic neutron scattering,^{13,15-17} and Mössbauer spectroscopy.¹¹ Among these methods, polarized Raman scattering is unique in that it can probe not only CF excitations but also scattering symmetries of the individual CF excitations. Information on the scattering symmetries enables one to properly assign transition characteristics of the CF excitations.¹⁴ Furthermore, Raman scattering can provide useful information on magnetic correlations to optical phonons. However, only a few papers using the Raman scattering technique have reported optical phonon behaviors in RNi_2B_2C for $R=Y, Ho,$ and Lu (Refs. 18-20), and CF excitations in ErNi₂B₂C.¹⁴ In this paper, we investigate CF excitations and optical phonon behaviors related to the AF order in DyNi₂B₂C.

II. EXPERIMENT

Raman scattering measurements were performed using a single-crystal DyNi₂B₂C sample² mounted inside a continuous He-flow cryostat. A 647.1-nm Kr-ion laser was focused on the sample in a backscattering geometry along the growth

(c axis) direction of the sample. Various polarization configurations were employed using linearly or circularly polarized light to identify the scattering symmetries for $\text{DyNi}_2\text{B}_2\text{C}$: $(\mathbf{E}_i, \mathbf{E}_s) = (x, x)$, $B_{1g} + A_{1g}$; (x, y) , $B_{2g} + A_{2g}$; (x', x') , $B_{2g} + A_{1g}$; (x', y') , $B_{1g} + A_{2g}$; (L, L) , $A_{1g} + A_{2g}$; and (L, R) , $B_{1g} + B_{2g}$, where \mathbf{E}_i and \mathbf{E}_s denote the incident and the analyzed polarization directions, respectively, and $x \parallel [1, 0, 0]$, $y \parallel [0, 1, 0]$, $z \parallel [0, 0, 1]$, $x' \parallel [1, 1, 0]$, and $y' \parallel [\bar{1}, 1, 0]$. Symbols L and R denote left and right circularly polarized light, respectively. B_{1g} , A_{1g} , B_{2g} , and A_{2g} are irreducible representations of the space group D_{4h} . Scattered light was dispersed using a triple-stage spectrometer and recorded using a liquid-nitrogen-cooled charge-coupled device (CCD) detector. After the CCD dark current response was removed from the raw spectra, a calibrated white light source was used to normalize the spectrometer response in order to correct the spectral artifacts due to the collection optics between the sample and the CCD detector. The corrected spectra were divided by the Bose thermal factor $[1 - \exp(-\hbar\omega/k_B T)]^{-1}$, giving rise to the Raman response proportional to the imaginary part of the Raman susceptibility.

III. RESULTS AND DISCUSSION

$\text{DyNi}_2\text{B}_2\text{C}$ single crystals have body-centered-tetragonal structure, belonging to space group $I4/mmm$ (D_{4h}^{17}). The ground state of the nine $4f$ electrons ($4f^9$) in Dy^{3+} is a 16-fold degenerate ${}^6H_{15/2}$ multiplet. The CF level splits the ground state multiplet into eight Kramers doublets within the D_{4h} site symmetry at the Dy site. Polarized Raman scattering is useful for identifying scattering symmetries of individual Raman modes. Figure 1(a) shows Raman spectra obtained at $T=4$ K in various polarization configurations. A strong mode at 199 cm^{-1} can be seen in the $B_{1g} + A_{2g}$, $B_{1g} + A_{1g}$, and $B_{1g} + B_{2g}$ Raman spectra, indicating that this mode has B_{1g} scattering symmetry. Indeed, the 199 cm^{-1} mode corresponds to the B_{1g} phonon mode from the c -axis Ni vibration.^{14,18,19} In addition to the Ni- B_{1g} phonon mode, three Raman modes are additionally observed at 124 , 151 , and 221 cm^{-1} . The sharp 124 cm^{-1} mode appears strongly in the $B_{1g} + A_{2g}$, $B_{1g} + A_{1g}$, and $B_{1g} + B_{2g}$ Raman spectra. Thus, this mode has mostly B_{1g} scattering symmetry. The 124 cm^{-1} mode also appears, though weakly, in the $A_{1g} + A_{2g}$ and the $B_{2g} + A_{2g}$ scattering symmetries. Consequently, the 124 cm^{-1} mode has a mixed characteristic of the B_{1g} and the A_{2g} scattering symmetries. A molecular field of $B=2.21$ T along the (110) direction in the commensurate AF state¹⁵ lowers the symmetry from D_{4h} to C_{2h} . Note that the twofold axis is along the (110) direction in C_{2h} . In this circumstance, the correlation table for D_{4h} tells us that both the B_{1g} and the A_{2g} symmetries become the B_g symmetry.²¹ Thus, the mixed B_{1g} and A_{2g} symmetries observed for the 124 cm^{-1} mode are most likely due to the presence of the molecular field in $\text{DyNi}_2\text{B}_2\text{C}$. The weak 151 cm^{-1} mode appears in the $B_{1g} + A_{2g}$ and the $B_{2g} + A_{2g}$ scattering symmetries. Thus, this mode has A_{2g} scattering symmetry. Similarly, the 221 cm^{-1} mode appears in the $B_{1g} + A_{2g}$, $B_{1g} + A_{1g}$, and $B_{1g} + B_{2g}$ Raman spectra, indicating that this mode has B_{1g} scattering symme-

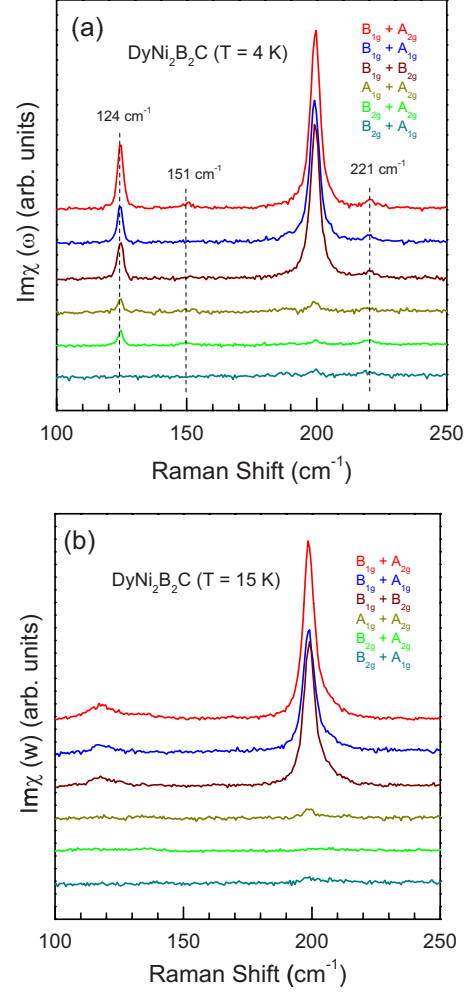


FIG. 1. (Color online) Polarized Raman spectra of $\text{DyNi}_2\text{B}_2\text{C}$ at (a) $T=4$ K and (b) $T=15$ K. From top to bottom, $(\mathbf{E}_i, \mathbf{E}_s) = (x', y')$, $B_{1g} + A_{2g}$; (x, x) , $B_{1g} + A_{1g}$; (L, R) , $B_{1g} + B_{2g}$; (L, L) , $A_{1g} + A_{2g}$; (x, y) , $B_{2g} + A_{2g}$; and (x', x') , $B_{2g} + A_{1g}$, respectively.

Figure 1(b) shows Raman spectra obtained at $T=15$ K in various polarization configurations. The linewidth of the Ni- B_{1g} phonon mode is broadened mostly due to spin-phonon interactions as well as thermal effect with increasing temperature through the AF ordering temperature. Temperature dependence of the Ni- B_{1g} phonon mode will be discussed in detail later. One noticeable feature in Fig. 1(b) is that the weak responses at 151 and 221 cm^{-1} , observed in the low temperature regime for $T < T_N$, disappear completely for $T > T_N = 10.3$ K. Note that, in contrast, the 124 cm^{-1} mode persists even for $T > T_N$. The quenching of the 151 and 221 cm^{-1} modes above the Néel temperature indicates the correlation of these modes to the commensurate AF order in $\text{DyNi}_2\text{B}_2\text{C}$, suggesting that these modes correspond to zone-folded phonons.²² Zone-folded phonons can appear when zone-boundary phonons are folded into the zone center due to the magnetic periodicity of $\text{DyNi}_2\text{B}_2\text{C}$ below the AF ordering temperature. The zone-folded phonons quench quickly with a disappearance of the magnetic periodicity above T_N . Such zone-folded phonons were previously observed in the commensurately ordered AF state in CuO .²³

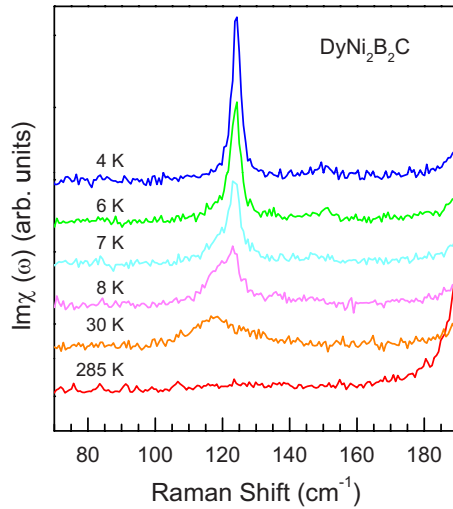


FIG. 2. (Color online) Temperature-dependent Raman spectra of $\text{DyNi}_2\text{B}_2\text{C}$ in $(\mathbf{E}_i, \mathbf{E}_s) = (x', y')$ scattering configuration.

The 124 cm^{-1} response appears very weakly and its line-width is significantly broadened at $T=15 \text{ K}$. Interestingly, in addition to the 124 cm^{-1} mode, a broad peak is newly observed at 119 cm^{-1} . The 119 cm^{-1} response is *not* a consequence of the thermal quenching of the 124 cm^{-1} mode with increasing temperature. As clearly shown in Fig. 1(b), the broad 119 cm^{-1} mode appears in the $B_{1g}+A_{2g}$, $B_{1g}+A_{1g}$, and $B_{1g}+B_{2g}$ Raman spectra, indicating that this excitation has B_{1g} scattering symmetry.

In order to identify the origins of the 124 cm^{-1} mode and the 119 cm^{-1} mode nearby, Raman spectra were carefully obtained as a function of temperature. Figure 2 shows the temperature evolution of the 124 and the 119 cm^{-1} modes. At very low temperatures ($T < 5 \text{ K}$), only the sharp peak at 124 cm^{-1} is observed. With increasing temperature above $T=5 \text{ K}$, the 124 cm^{-1} response decreases in intensity and broadens in spectral width. Interestingly, a broad response at 119 cm^{-1} appears at the lower frequency region of this sharp mode. Figure 3(a) shows a representative Raman spectrum at $T=8 \text{ K}$, together with the fitting curves, that clearly exhibits the coexistence of the 124 and the 119 cm^{-1} modes. The intensity and spectral width changes extracted by fitting the individual Raman spectra to a Lorentzian line shape for the 119 and the 124 cm^{-1} modes are summarized in Figs. 3(b) and 3(c), respectively. With increasing temperature further above $T=10 \text{ K}$, the 124 cm^{-1} response decreases rapidly in intensity. Furthermore, spectral width becomes significantly broadened. The rapid decrease in intensity of the sharp response near $T=10 \text{ K}$ may indicate the correlation of the 124 cm^{-1} mode to the commensurate AF order in $\text{DyNi}_2\text{B}_2\text{C}$, suggesting that the 124 cm^{-1} mode can be related to a zone-folded optical phonon. However, this assumption is unlikely to be correct. The temperature-dependent behaviors, i.e., thermal quenching and linewidth broadening upon raising temperature, of the 124 cm^{-1} response suggest that this mode corresponds to a CF excitation.¹⁴ Indeed, inelastic neutron scattering from $\text{DyNi}_2\text{B}_2\text{C}$ revealed a CF transition around 15 meV (121 cm^{-1}),¹⁵ which is very close to the peak energy (124 cm^{-1}) of the sharp mode observed

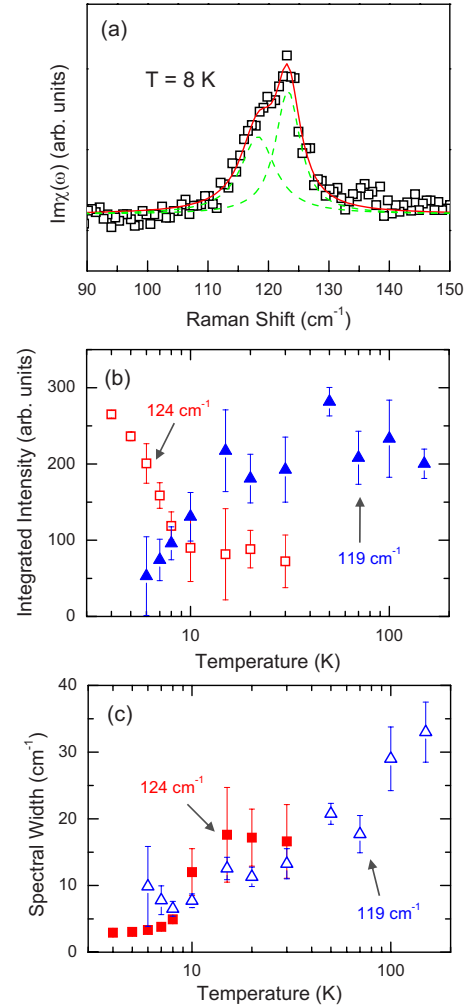


FIG. 3. (Color online) (a) A representative Raman spectrum (open squares) at $T=8 \text{ K}$ with individual fitting results (dashed lines) for the 119 and the 124 cm^{-1} modes. A solid line indicates a fitted result to a Lorentzian line shape. (b) Intensity and (c) spectral width changes as a function of temperature for the 119 and the 124 cm^{-1} modes.

in our results. Thus, we attribute the peak at 124 cm^{-1} to a CF excitation. The 119 and the 124 cm^{-1} responses coexist in the temperature regime for $6 \text{ K} \leq T \leq 30 \text{ K}$. Figure 2 shows that the 124 cm^{-1} response at 30 K , on the high-frequency side of the 119 cm^{-1} mode, is significantly weakened and exhibits significantly broadened line shape. When the temperature is higher than 30 K , only the broad response at 119 cm^{-1} appears in the Raman spectrum. While the 124 cm^{-1} mode rapidly diminishes in intensity with increasing temperature, the broad 119 cm^{-1} mode grows in intensity as temperature is further increased from 6 to 50 K . The 119 cm^{-1} mode gradually diminishes in intensity with increasing temperature further above $T=50 \text{ K}$, and is hardly observable for $T > 150 \text{ K}$. Both the 119 and the 124 cm^{-1} modes are broadened systematically in spectral width with increasing temperature.

Using the CF Hamiltonian and CF parameters for $\text{DyNi}_2\text{B}_2\text{C}$, Gasser *et al.*^{13,15} calculated a low-lying Kramers doublet at about 0.3 meV (2.4 cm^{-1}). In addition, an inelas-

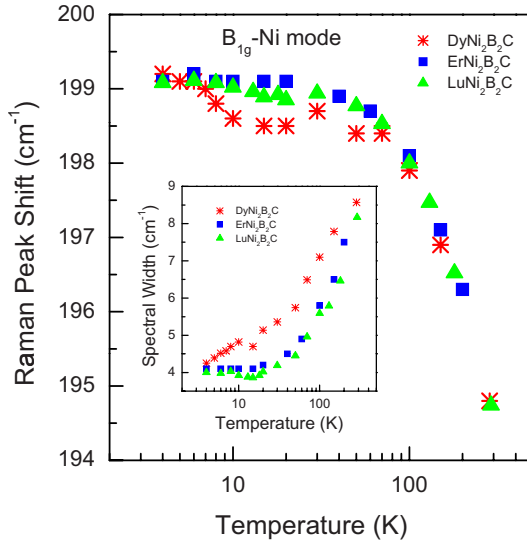


FIG. 4. (Color online) Temperature evolution of the Raman peak energies of the Ni- B_{1g} phonons for DyNi₂B₂C (asterisks), ErNi₂B₂C (solid squares), and LuNi₂B₂C (solid triangles). The inset shows spectral width changes as a function of temperature of the Ni- B_{1g} phonons for DyNi₂B₂C (asterisks), ErNi₂B₂C (solid squares), and LuNi₂B₂C (solid triangles).

tic neutron scattering study of Dy_{0.05}Lu_{0.95}Ni₂B₂C revealed a low-lying CF transition at 0.2 meV (1.6 cm⁻¹) at $T = 1.8$ K.²⁴ The intensity of the low-lying CF transition at 0.2 meV diminishes rapidly with increasing temperature due to a line broadening caused by thermal population of this energy level.²⁴ Thus, if we assume that a low-lying CF transition exists at 5 cm⁻¹ in DyNi₂B₂C and that this CF level is rapidly thermally saturated at higher temperatures, similar to the case of Dy_{0.05}Lu_{0.95}Ni₂B₂C, the 119 cm⁻¹ mode can be attributed to the excited CF transition from the low-lying level at 5 cm⁻¹ to the CF level at 124 cm⁻¹. Indeed, as described previously, the temperature dependence of the 119 cm⁻¹ response in both intensity and linewidth strongly suggests that this mode corresponds to an excited CF transition. Thermal saturation of the ground-state low-lying level (~ 5 cm⁻¹) probably initiates an excited CF transition from this low-lying level to the higher level at 124 cm⁻¹. Activation of the 119 cm⁻¹ excitation at higher temperatures may suppress the CF level transition at 124 cm⁻¹, giving rise to a rapid diminishment in intensity with increasing temperature, as shown in the intensity changes illustrated in Fig. 3(b). This scenario also validates the assignment of the 124 cm⁻¹ mode as a CF excitation. Inelastic neutron-scattering studies revealed similar behaviors of the excited CF transitions in Pr₂CuO₄ (Ref. 16) and PrNi₂B₂C.¹⁷

Now we focus on the Ni- B_{1g} mode at 199 cm⁻¹. As summarized in Fig. 4, this mode exhibits anomalous temperature-dependent behaviors both in peak shift and in spectral width, i.e., with increasing T toward T_N , both a downward shift of the peak energy and a broadening of the

spectral width are enhanced in the vicinity of T_N . Furthermore, the spectral widths of the Ni- B_{1g} modes in DyNi₂B₂C are much broader in all temperature ranges than those in both LuNi₂B₂C and ErNi₂B₂C. The anomalous temperature dependence of the Ni- B_{1g} mode near T_N suggests that this phonon mode strongly couples to the AF order in DyNi₂B₂C. In contrast, as shown in Fig. 4, we did not observe any temperature-dependent phonon anomalies in nonmagnetic LuNi₂B₂C ($T_c = 16.6$ K) nor in magnetic ErNi₂B₂C ($T_N = 6$ K, $T_c = 10$ K). Similar anomalous phonon-energy changes in the vicinity of the AF ordering temperature were previously reported for several AF compounds such as MnTe ($T_N \sim 307$ K),²⁵ YCrO₃ ($T_N \sim 141$ K), and GdCrO₃ ($T_N \sim 170$ K).²⁶ In nonsuperconducting GdSr₂RuCu₂O₈, an enhancement of the phonon energies below the magnetic ordering temperature (~ 140 K) was attributed to the presence of strong spin-phonon interactions in this compound.²⁷ Recently, Raman scattering from magnetic superconductor RuSr₂(Eu_{1.5}Ce_{0.5})Cu₂O₁₀ revealed that some phonon modes exhibited anomalous softening and spectral width broadening below 100 K.²⁸ This anomalous phonon-mode behavior is attributed to spin-phonon interactions.²⁸ All of these results unambiguously demonstrate that the onset of magnetic order can strongly couple to phonons. Thus, the anomalous temperature-dependent behavior of the Ni- B_{1g} mode near T_N in DyNi₂B₂C is most likely due to the spin-phonon correlation in the vicinity of T_N .²⁹

IV. CONCLUSIONS

In conclusion, polarized Raman spectra from DyNi₂B₂C revealed a Ni- B_{1g} mode at 199 cm⁻¹ and additional modes at 124, 151, and 221 cm⁻¹. The 124 cm⁻¹ mode exhibits mostly B_{1g} scattering symmetry. The 151 and 221 cm⁻¹ modes exhibit A_{2g} and B_{1g} scattering symmetries, respectively. Rapid quenching of both the 151 and 221 cm⁻¹ modes below the AF ordering temperature suggests that these modes correspond to zone-folded phonons. The 124 cm⁻¹ mode is attributed to CF excitation, as evidenced by temperature-dependent behaviors in its intensities and spectral widths. The 119 cm⁻¹ mode observed at higher temperatures corresponds to an excited CF transition. The enhancement in both the linewidth broadening and the peak-energy decrease in the Ni- B_{1g} mode at 199 cm⁻¹ in the vicinity of T_N indicates that strong spin-phonon interactions are present in DyNi₂B₂C. Our results demonstrate that Raman scattering studies can provide rich information on the CF excitations, optical phonons, and their spin correlations.

ACKNOWLEDGMENTS

H.R. acknowledges financial support by Mid-career Researcher Program through NRF grant funded by the MEST (Grant No. 2009-0083859). Work at the Ames Laboratory was supported by the Department of Energy, Basic Energy Sciences under Contract No. DE-AC02-07CH11358.

*rho@chonbuk.ac.kr

- ¹P. C. Canfield, P. L. Gammel, and D. J. Bishop, *Phys. Today* **51**, 40 (1998).
- ²B. K. Cho, P. C. Canfield, and D. C. Johnston, *Phys. Rev. B* **52**, R3844 (1995).
- ³B. K. Cho, B. N. Harmon, D. C. Johnston, and P. C. Canfield, *Phys. Rev. B* **53**, 2217 (1996).
- ⁴B. K. Cho, P. C. Canfield, L. L. Miller, D. C. Johnston, W. P. Beyermann, and A. Yatskar, *Phys. Rev. B* **52**, 3684 (1995).
- ⁵B. K. Cho, M. Xu, P. C. Canfield, L. L. Miller, and D. C. Johnston, *Phys. Rev. B* **52**, 3676 (1995).
- ⁶B. K. Cho, P. C. Canfield, and D. C. Johnston, *Phys. Rev. Lett.* **77**, 163 (1996).
- ⁷P. C. Canfield, B. K. Cho, D. C. Johnston, D. K. Finnemore, and M. F. Hundley, *Physica C* **230**, 397 (1994).
- ⁸H. Eisaki, H. Takagi, R. J. Cava, B. Batlogg, J. J. Krajewski, W. F. Peck, K. Mizuhashi, J. O. Lee, and S. Uchida, *Phys. Rev. B* **50**, 647 (1994).
- ⁹B. D. Dunlap, L. N. Hall, F. Behroozi, G. W. Crabtree, and D. G. Niarchos, *Phys. Rev. B* **29**, 6244 (1984).
- ¹⁰J. W. Lynn, S. Skanthakumar, Q. Huang, S. K. Sinha, Z. Hossain, L. C. Gupta, R. Nagarajan, and C. Godart, *Phys. Rev. B* **55**, 6584 (1997).
- ¹¹J. P. Sanchez, P. Vulliet, C. Godart, L. C. Gupta, Z. Hossain, and R. Nagarajan, *Phys. Rev. B* **54**, 9421 (1996).
- ¹²S. Jandl, T. Strach, T. Ruf, M. Cardona, V. Nekvasil, M. Iliev, D. I. Zhigunov, S. N. Barilo, and S. V. Shiryaev, *Phys. Rev. B* **56**, 5049 (1997).
- ¹³U. Gasser, P. Allenspach, F. Fauth, W. Henggeler, J. Mesot, A. Furrer, S. Rosenkranz, P. Vorderwisch, and M. Buchgeister, *Z. Phys. B* **101**, 345 (1996).
- ¹⁴H. Rho, M. V. Klein, and P. C. Canfield, *Phys. Rev. B* **69**, 144420 (2004).
- ¹⁵U. Gasser, P. Allenspach, and A. Furrer, *Physica B* **241-243**, 789 (1998).
- ¹⁶P. Allenspach, S.-W. Cheong, A. Dommann, P. Fischer, Z. Fisk, A. Furrer, H. R. Ott, and B. Rupp, *Z. Phys. B* **77**, 185 (1989).
- ¹⁷Chandan Mazumdar, M. Rotter, M. Frontzek, H. Michor, M. Doerr, A. Kreyssig, M. Koza, A. Hiess, J. Voigt, G. Behr, L. C. Gupta, M. Prager, and M. Loewenhaupt, *Phys. Rev. B* **78**, 144422 (2008).
- ¹⁸V. G. Hadjiev, L. N. Bozukov, and M. G. Baychev, *Phys. Rev. B* **50**, 16726 (1994).
- ¹⁹H.-J. Park, H.-S. Shin, H.-G. Lee, I.-S. Yang, W. C. Lee, B. K. Cho, P. C. Canfield, and D. C. Johnston, *Phys. Rev. B* **53**, 2237 (1996).
- ²⁰T. Hirata and H. Takeya, *Phys. Rev. B* **57**, 2671 (1998).
- ²¹W. G. Fateley, F. R. Dollish, N. T. McDevitt, and F. F. Bentley, *Infrared and Raman Selection Rules for Molecular and Lattice Vibrations: The Correlation Method* (Wiley, New York, 1972).
- ²²The possibility of these modes coming from the CF or magnon excitations cannot be ruled out.
- ²³X. K. Chen, J. C. Irwin, and J. P. Franck, *Phys. Rev. B* **52**, R13130 (1995).
- ²⁴M. Rotter, C. Sierks, M. Loewenhaupt, J. Freudenberger, and H. Schober, in *Rare Earth Transition Metal Borocarbides (Nitrides): Superconducting, Magnetic and Normal State Properties*, edited by K.-H. Muller and V. Narozhnyi (Kluwer Academic Publishers, The Netherlands, 2001), p. 137.
- ²⁵S. Onari, T. Arai, and K. Kudo, *Solid State Commun.* **14**, 507 (1974).
- ²⁶M. Udagawa, K. Kohn, N. Koshizuka, T. Tsushima, and K. Tsushima, *Solid State Commun.* **16**, 779 (1975).
- ²⁷V. G. Hadjiev, J. Backstrom, V. N. Popov, M. N. Iliev, R. L. Meng, Y. Y. Xue, and C. W. Chu, *Phys. Rev. B* **64**, 134304 (2001).
- ²⁸V. G. Sathe, V. P. S. Awana, A. Deshpande, H. Kishan, and A. V. Narlikar, *Solid State Commun.* **141**, 658 (2007).
- ²⁹In addition, DyNi₂B₂C is likely to be nonuniform in its local magnetic properties. Further, the possibility remains that CF excitations may exist at energies comparable to the phonon energy that might couple to the phonon due to broken symmetry.